



Integration of Remote Sensing and Deep Learning for Forest Fire Risk Mapping

**Dr. Auti Sharad Karna Saheb¹, Dr. Wagh Rajesh Vasantrao², Dr. Balu Laxman Rathod³,
Dr. Ranjana H. Rathod⁴**

¹ Associate Professor, Department of Geography, Arts, Commerce and Science College, Sonai, Tal. Newasa, Dist. Ahilyanagar

² Associate Professor, Department of Geography, Shri Dnyaneshwar Mahavidyalaya, Newasa, Tal. Newasa, Dist. Ahilyanagar

³ Associate Professor, Department of Geography, Kankavli College, Kankavli, Dist. Sindhudurg – 416602

⁴ Assistant Professor, Department of Geography, Nowrosjee Wadia College, Pune
E-mail: skauti14@gmail.com¹, rajeshwagh2424@gmail.com², balurathod267@gmail.com³,
ranjanarathodwadia@gmail.com⁴

Abstract

Forest fires have emerged as one of the most critical environmental hazards, causing extensive ecological degradation, biodiversity loss, carbon emissions, and socioeconomic disruptions across forested landscapes worldwide. Accurate forest fire risk mapping is therefore essential for supporting early warning systems, resource allocation, and sustainable forest management. Recent advances in Earth observation technologies have enabled the continuous acquisition of multisource remote sensing data, while deep learning techniques have demonstrated superior capabilities in extracting complex spatial and temporal patterns from large geospatial datasets. This paper investigates the integration of remote sensing and deep learning methodologies for forest fire risk mapping by utilizing satellite-derived environmental variables, including vegetation indices, land surface temperature, topography, meteorological parameters, and land-cover characteristics. The study evaluates the effectiveness of deep neural architectures in modeling nonlinear relationships between fire occurrence and contributing factors. Furthermore, a comprehensive framework is proposed to enhance prediction accuracy, spatial generalization, and operational applicability for wildfire management. The findings highlight the potential of synergizing remote sensing observations with advanced deep learning models to improve fire susceptibility assessment, support decision-making processes, and strengthen disaster preparedness strategies under changing climatic conditions.

Keywords: Forest Fire Risk Mapping, Remote Sensing, Deep Learning, Wildfire Prediction, Geospatial Analytics, Environmental Monitoring

1. Introduction

Forest fires constitute one of the most destructive natural hazards affecting terrestrial ecosystems across the globe. Their occurrence has increased considerably during recent decades due to the combined influences of climate change, prolonged drought conditions, land-use modifications, and anthropogenic interventions. Wildfires not only result in extensive vegetation loss and habitat destruction but also contribute significantly to atmospheric greenhouse gas emissions, soil degradation, hydrological imbalance, and socioeconomic losses. The increasing frequency and intensity of forest fire events have elevated the necessity for developing reliable and accurate fire risk assessment frameworks capable of supporting preventive management and emergency response strategies. The emergence of advanced Earth observation technologies has transformed the manner in which forest ecosystems are monitored and analyzed. Satellite-based remote sensing platforms provide continuous, large-scale, and cost-effective observations of environmental conditions associated with fire occurrence. Simultaneously, recent developments in artificial intelligence, particularly deep learning, have enabled researchers to model highly complex and nonlinear relationships among environmental variables. The integration of remote sensing data with deep learning techniques has therefore become a promising research direction for improving the accuracy and efficiency of forest fire risk mapping.

Overview

Forest fire risk mapping refers to the spatial identification and classification of regions according to their likelihood of experiencing fire incidents. Traditional fire risk assessment methods primarily relied on statistical approaches, expert knowledge, and geographic information systems (GIS)-based multicriteria evaluation techniques. Although these methods have contributed significantly to wildfire management practices, their ability to capture complex interactions among environmental factors remains limited. Remote sensing technologies offer valuable information regarding vegetation health, fuel availability, moisture conditions, topographic characteristics, land surface temperature, and meteorological dynamics. Modern satellite missions such as Landsat, Sentinel, MODIS, and VIIRS provide high-resolution datasets that facilitate near-real-time environmental monitoring. These datasets have become essential resources for wildfire prediction and susceptibility assessment.

Deep learning methodologies have demonstrated remarkable performance in extracting hierarchical features from large and heterogeneous datasets. Architectures such as Convolutional Neural Networks (CNNs), Recurrent Neural Networks (RNNs), Long Short-Term Memory (LSTM) networks, Autoencoders, and hybrid models are increasingly employed for geospatial prediction tasks. Their capability to automatically learn spatial and temporal representations makes them particularly suitable for forest fire risk modeling. Consequently, integrating remote sensing observations with deep learning algorithms provides a comprehensive framework capable of improving predictive performance, reducing uncertainty, and generating highly accurate forest fire risk maps. Such integration supports proactive disaster management by identifying vulnerable areas before fire outbreaks occur.

Scope and Objectives

The scope of this paper encompasses the investigation of remote sensing datasets and deep learning methodologies for forest fire risk mapping. The study focuses on identifying key environmental variables influencing wildfire occurrence and examining the effectiveness of advanced deep learning architectures in modeling fire susceptibility patterns.

The primary objectives of this paper are:

1. To examine the role of remote sensing technologies in forest fire monitoring and risk assessment.
2. To analyze major environmental and geospatial factors contributing to wildfire occurrence.
3. To investigate deep learning architectures applicable to forest fire prediction and susceptibility mapping.
4. To develop an integrated framework combining remote sensing data and deep learning techniques.
5. To evaluate the effectiveness of the proposed framework for generating accurate forest fire risk maps.
6. To identify future research opportunities for improving wildfire prediction systems under changing climatic conditions.

Author Motivations

The growing environmental and socioeconomic consequences associated with wildfire disasters have motivated the exploration of advanced computational approaches for risk assessment. Conventional methods often face limitations in handling high-dimensional geospatial datasets and nonlinear environmental interactions. Meanwhile, remote sensing technologies continuously generate massive volumes of spatial information that remain underutilized in many operational fire management systems.

Recent breakthroughs in deep learning provide unprecedented opportunities for extracting meaningful patterns from multisource geospatial data. The motivation behind this study is to bridge the gap between Earth observation capabilities and intelligent predictive modeling techniques by proposing an integrated framework capable of supporting more effective wildfire prevention and management strategies.

Furthermore, the increasing availability of open-access satellite datasets and computational resources creates favorable conditions for implementing scalable and transferable fire risk mapping systems. This paper seeks to contribute to this evolving research domain by synthesizing current knowledge and identifying pathways for future advancement.

Paper Structure

This paper is organized into seven major sections. Section 1 introduces the background, significance, objectives, and motivation of the study. Section 2 presents a comprehensive review of existing literature related to remote sensing, machine learning, and deep learning applications in forest fire risk mapping. Section 3 discusses remote sensing data sources and major fire-conditioning factors influencing wildfire susceptibility. Section 4 describes deep learning architectures and modeling frameworks applicable to forest fire prediction. Section 5 proposes an integrated methodology for combining remote sensing datasets with deep learning techniques and outlines validation procedures. Section 6 analyzes risk zonation outcomes and discusses practical implications for disaster management and policy formulation. Finally, Section 7 summarizes key findings, limitations, and future research directions.

The integration of remote sensing technologies and deep learning methodologies represents a transformative advancement in forest fire risk assessment. By leveraging the complementary strengths of continuous Earth observation and intelligent feature learning, researchers and decision-makers can develop more accurate, scalable, and operationally effective wildfire management systems. As climate-induced fire risks continue to intensify globally, the development of robust predictive frameworks will become increasingly important for safeguarding ecosystems, biodiversity, human settlements, and sustainable environmental resources.

2. Literature Review with Research Gap

Forest fire risk mapping has evolved significantly over the past two decades, transitioning from traditional statistical analyses and expert-based assessments toward data-driven and artificial intelligence-based approaches. The rapid growth of satellite remote sensing technologies, combined with advances in machine learning and deep learning, has enabled the development of sophisticated wildfire prediction systems capable of analyzing complex environmental interactions. Existing literature demonstrates substantial progress in integrating geospatial information with computational intelligence techniques; however, several methodological and operational challenges remain unresolved.

Remote sensing has become a fundamental component of wildfire monitoring and risk assessment due to its capability to provide repetitive, large-scale, and objective observations of terrestrial environments. Recent studies have emphasized the importance of multispectral and thermal satellite datasets for detecting environmental

conditions associated with wildfire occurrence. Chuvieco, Yebra, Jurdao, Aguado, Koutsias, and Martínez [10] highlighted the growing role of Earth observation technologies in fire danger assessment through the utilization of vegetation condition indicators, fuel moisture estimates, and land surface temperature measurements. Similarly, Pérez-Cabello, Montorio Llovería, García-Martín, and de Luis [9] demonstrated that remote sensing platforms significantly enhance the monitoring of fire-prone landscapes by facilitating the extraction of critical environmental variables relevant to wildfire susceptibility.

Several researchers have investigated the application of machine learning techniques for forest fire susceptibility mapping. Pourghasemi, Gayen, Edalat, Tiefenbacher, and Ismail [8] evaluated multiple machine learning algorithms using geospatial datasets and reported considerable improvements in predictive accuracy compared with conventional statistical methods. Their findings indicated that machine learning algorithms effectively capture nonlinear relationships among fire conditioning factors such as elevation, slope, vegetation density, temperature, and precipitation.

Similarly, Mohajane, Costache, Karimi, Pham, Essahlaoui, and Oudija [5] conducted a comparative assessment of machine learning techniques for wildfire susceptibility mapping and concluded that ensemble and intelligent learning approaches consistently outperform traditional classification methods. Their study emphasized the importance of integrating diverse environmental variables derived from remote sensing datasets to enhance model robustness.

Recent research has increasingly shifted toward deep learning-based methodologies due to their superior capability in automatic feature extraction and hierarchical representation learning. Bisquert, Caselles, Sánchez, and Caselles [7] demonstrated that deep learning models significantly improve wildfire danger forecasting by effectively learning complex spatial patterns from Earth observation datasets. Their study highlighted the advantages of deep neural networks over shallow machine learning algorithms in handling large-scale geospatial information.

The emergence of convolutional neural networks has attracted substantial attention within wildfire prediction research. CNN-based architectures are particularly effective in capturing spatial dependencies within satellite imagery. Sharma, Singh, Kumar, and Jain [2] developed a convolutional neural network framework utilizing satellite-derived environmental variables and reported notable improvements in wildfire prediction performance. Their findings suggested that CNNs can successfully identify spatial signatures associated with high-risk fire zones.

The integration of Sentinel-2 imagery with deep learning techniques has also gained prominence. González, Martínez, Rodríguez, and Pérez [3] investigated the use of deep neural networks for wildfire risk assessment in Mediterranean ecosystems. Their research demonstrated that high-resolution multispectral imagery substantially improves the detection of vegetation stress conditions and fuel characteristics associated with fire occurrence. The study further revealed that deep learning models outperform conventional approaches in terms of classification accuracy and spatial generalization.

Hybrid deep learning frameworks have emerged as another significant research direction. Wang, Zhao, Sun, and Guo [4] proposed a hybrid deep learning model integrating remote sensing data and GIS-derived variables for wildfire susceptibility mapping. Their results indicated that combining multiple deep learning architectures enhances predictive stability and reduces uncertainty associated with individual models. The study highlighted the potential of hybrid frameworks for generating more reliable fire risk maps across heterogeneous landscapes.

Explainable artificial intelligence has recently been introduced to address the interpretability limitations of deep learning models. Zhang, Li, Wang, Chen, and Liu [1] integrated explainable AI mechanisms with deep neural networks to improve transparency in wildfire susceptibility mapping. Their study demonstrated that explainable frameworks enable researchers and decision-makers to identify dominant environmental drivers influencing fire occurrence, thereby enhancing trust and practical applicability.

Furthermore, Jaafari, Bin Ahmad, Pham, Kheirkhah Zarkesh, Chapi, and Shahabi [6] investigated wildfire probability mapping using remote sensing and machine learning algorithms. Their findings confirmed that environmental variables derived from satellite observations significantly contribute to predictive performance. The study emphasized the necessity of integrating topographic, climatic, and vegetation-related parameters for comprehensive fire susceptibility assessment.

A common trend observed across the literature is the increasing reliance on multisource datasets for wildfire prediction. Researchers consistently utilize combinations of vegetation indices, land surface temperature, digital elevation models, rainfall patterns, wind characteristics, soil moisture indicators, and land-use information to improve model performance [1], [2], [4], [5]. The availability of high-resolution satellite imagery has further facilitated the development of spatially detailed fire risk maps suitable for operational management applications. Despite substantial advancements, several research challenges remain. First, many existing studies focus on region-specific datasets, limiting the transferability and generalization capability of developed models [2], [3], [5]. Second, deep learning architectures often function as black-box systems, reducing interpretability and limiting acceptance among decision-makers [1]. Third, the integration of temporal dynamics within fire prediction models remains insufficiently explored, particularly for long-term risk assessment [7]. Fourth, variations in spatial resolution, sensor characteristics, and environmental conditions introduce significant uncertainty in model performance across different geographical regions [4], [8]. Fifth, relatively few studies have investigated unified frameworks that simultaneously incorporate multisource remote sensing data, deep learning architectures, explainability mechanisms, and operational validation procedures [1], [4].

Research Gap

A critical analysis of existing literature reveals that although remote sensing and deep learning have independently demonstrated significant potential for forest fire risk assessment, their integrated utilization remains insufficiently optimized. Most previous studies concentrate on either specific satellite datasets or individual deep learning architectures without comprehensively addressing multisource data fusion, temporal variability, and model interpretability [1]–[8]. Furthermore, limited attention has been devoted to developing scalable and transferable frameworks capable of operating across diverse ecological and climatic conditions. Existing models also exhibit challenges related to explainability, uncertainty quantification, and real-time operational deployment. Therefore, there exists a substantial research gap in designing an integrated remote sensing–deep learning framework that combines heterogeneous environmental datasets, advanced feature learning capabilities, explainable prediction mechanisms, and robust validation strategies for accurate and operationally applicable forest fire risk mapping. Such a framework has the potential to significantly improve wildfire preparedness, risk mitigation, and sustainable forest management practices.

3. Remote Sensing Data Sources and Forest Fire Conditioning Factors

Forest fire occurrence is governed by a complex interaction among climatic, topographic, vegetation, anthropogenic, and environmental variables. Accurate fire risk mapping therefore requires the integration of multiple geospatial datasets capable of representing these factors at adequate spatial and temporal resolutions. Remote sensing technologies provide a robust platform for acquiring such information continuously across extensive geographical regions. Modern Earth observation satellites enable the derivation of numerous fire-conditioning factors that can be incorporated into deep learning models for predictive risk assessment.

The present framework integrates multisource remote sensing datasets obtained from optical, thermal, radar, and meteorological satellites. These datasets collectively characterize vegetation health, fuel availability, surface temperature dynamics, moisture conditions, terrain morphology, and human influence patterns that contribute to wildfire ignition and propagation.

3.1 Remote Sensing Data Sources

Several satellite missions have become indispensable for forest fire monitoring and susceptibility assessment.

Table 1: Major Remote Sensing Datasets Used for Forest Fire Risk Mapping

Satellite/Sensor	Spatial Resolution	Temporal Resolution	Key Variables
Sentinel-2 MSI	10-20 m	5 days	NDVI, NBR, Land Cover
Landsat-8/9 OLI-TIRS	30 m	16 days	LST, Vegetation Indices
MODIS	250-1000 m	Daily	Active Fire, NDVI
VIIRS	375 m	Daily	Fire Detection
Sentinel-1 SAR	10 m	6-12 days	Surface Moisture
ERA5 Climate Data	0.25°	Hourly	Temperature, Wind, Rainfall

Table 1 summarizes the principal remote sensing datasets utilized for forest fire risk analysis.

The integration of multisensor observations provides complementary information regarding environmental conditions associated with fire susceptibility. Optical sensors capture vegetation characteristics, thermal sensors monitor heat anomalies, while radar systems estimate moisture content regardless of cloud cover conditions.

3.2 Vegetation-Based Fire Conditioning Factors

Vegetation acts as the primary fuel source for wildfire events. Consequently, spectral vegetation indices derived from satellite imagery play a crucial role in fire risk assessment.

Normalized Difference Vegetation Index (NDVI)

NDVI measures vegetation vigor and photosynthetic activity.

$$NDVI = \frac{NIR - Red}{NIR + Red}$$

where:

- *NIR* = Near Infrared reflectance
- *Red* = Red band reflectance

NDVI values range from -1 to +1. Higher values indicate dense vegetation, whereas lower values correspond to sparse vegetation or degraded ecosystems.

Enhanced Vegetation Index (EVI)

EVI improves vegetation monitoring under dense canopy conditions.

$$EVI = G \frac{(NIR - Red)}{(NIR + C_1 Red - C_2 Blue + L)}$$

where:

- *G* = 2.5
- *L* = 1
- *C*₁ = 6
- *C*₂ = 7.5

Normalized Burn Ratio (NBR)

NBR is highly effective for detecting burned areas and fuel conditions.

$$NBR = \frac{NIR - SWIR}{NIR + SWIR}$$

where SWIR represents Short-Wave Infrared reflectance.

Table 2: Vegetation Indicators and Their Fire Risk Significance

Indicator	Description	Fire Risk Implication
NDVI	Vegetation Density	Fuel Availability
EVI	Canopy Structure	Biomass Estimation
NBR	Burn Severity	Fuel Dryness
SAVI	Soil Adjusted Vegetation Index	Sparse Vegetation Analysis
NDMI	Moisture Index	Fuel Moisture Assessment

Table 2 illustrates the relationship between vegetation indices and forest fire susceptibility.

3.3 Thermal Factors

Surface temperature directly influences fuel desiccation and ignition probability.

Land Surface Temperature (LST)

LST is estimated from thermal infrared observations.

$$LST = \frac{BT}{1 + \left(\frac{\lambda BT}{\rho}\right) \ln \varepsilon}$$

where:

- BT = Brightness Temperature
- λ = Wavelength
- $\rho = 1.438 \times 10^{-2}$
- ε = Surface Emissivity

Elevated LST values indicate increased fire susceptibility due to reduced vegetation moisture.

Fire Radiative Power (FRP)

FRP quantifies heat energy released during combustion.

$$FRP = \sigma T^4 A$$

where:

- σ = Stefan-Boltzmann Constant
- T = Temperature
- A = Burning Area

High FRP values indicate intense wildfire activity.

3.4 Topographic Factors

Terrain characteristics strongly influence wildfire ignition and spread dynamics.

Slope

Slope affects fire propagation velocity.

$$Slope = \tan^{-1} \left(\sqrt{\left(\frac{\partial z}{\partial x}\right)^2 + \left(\frac{\partial z}{\partial y}\right)^2} \right)$$

Steeper slopes generally facilitate faster uphill fire spread.

Aspect

Aspect determines solar radiation exposure.

$$Aspect = \tan^{-1} \left(\frac{\partial z / \partial y}{-\partial z / \partial x} \right)$$

South-facing slopes typically experience higher temperatures and lower moisture content.

Elevation

Elevation influences atmospheric conditions and vegetation composition.

Table 3: Topographic Variables for Fire Susceptibility Assessment

Variable	Unit	Impact on Fire Risk
Elevation	m	Climate Variation
Slope	Degree	Fire Spread Speed
Aspect	Degree	Solar Exposure
Curvature	Dimensionless	Water Accumulation
Terrain Ruggedness	Index	Accessibility and Spread

Table 3 presents major topographic conditioning factors utilized in forest fire risk modeling.

3.5 Meteorological Factors

Weather conditions represent dynamic drivers of wildfire occurrence.

Relative Humidity

$$RH = \frac{e}{e_s} \times 100$$

where:

- e = Actual Vapor Pressure
- e_s = Saturation Vapor Pressure

Lower relative humidity significantly increases fire risk.

Wind Speed Influence

Fire spread rate can be represented as:

$$R = R_0 e^{kW}$$

where:

- R = Fire Spread Rate
- R_0 = Base Spread Rate
- W = Wind Speed
- k = Wind Coefficient

Fire Weather Index (FWI)

$$FWI = f(T, RH, W, P)$$

where:

- T = Temperature
- RH = Relative Humidity
- W = Wind Speed
- P = Precipitation

FWI integrates multiple meteorological variables into a unified fire danger indicator.

3.6 Anthropogenic Factors

Human activities are responsible for a substantial proportion of wildfire ignitions worldwide.

Important anthropogenic variables include:

- Distance from roads
- Distance from settlements
- Population density
- Agricultural activity
- Tourism pressure
- Infrastructure development

Distance from roads can be calculated as:

$$D_r = \sqrt{(x - x_r)^2 + (y - y_r)^2}$$

where x_r, y_r denote road coordinates.

3.7 Feature Integration and Risk Variable Matrix

All environmental variables are integrated into a multidimensional feature matrix.

$$X = \begin{bmatrix} x_{11} & x_{12} & \cdots & x_{1n} \\ x_{21} & x_{22} & \cdots & x_{2n} \\ \vdots & \vdots & \ddots & \vdots \\ x_{m1} & x_{m2} & \cdots & x_{mn} \end{bmatrix}$$

where:

- m = number of spatial samples
- n = number of conditioning variables

The resulting feature matrix serves as the primary input for deep learning-based forest fire risk modeling discussed in the subsequent section.

4. Deep Learning Framework for Forest Fire Risk Modeling

The increasing availability of large-scale geospatial datasets has transformed forest fire risk assessment from traditional statistical modeling toward advanced deep learning paradigms capable of extracting complex spatial and temporal relationships from heterogeneous environmental variables. Unlike conventional machine learning approaches that require manual feature engineering, deep learning architectures automatically learn hierarchical representations from raw data, thereby improving predictive performance and generalization capabilities.

In forest fire risk mapping, deep learning models are trained using multisource remote sensing variables, meteorological observations, topographic information, and anthropogenic factors. The objective is to learn nonlinear interactions among these variables and classify each spatial location according to its wildfire susceptibility level.

The proposed framework incorporates Convolutional Neural Networks (CNN), Long Short-Term Memory (LSTM) networks, Residual Networks (ResNet), Attention Mechanisms, and Hybrid CNN-LSTM architectures to capture both spatial and temporal dependencies associated with wildfire occurrence.

4.1 Deep Learning Architecture Overview

The proposed architecture consists of five sequential stages:

1. Data Acquisition
2. Data Preprocessing
3. Feature Extraction
4. Deep Learning Training
5. Risk Classification and Mapping

Table 4: Deep Learning Components in Forest Fire Risk Mapping

Component	Function
CNN	Spatial Feature Extraction
LSTM	Temporal Dependency Learning
ResNet	Deep Feature Representation
Attention Layer	Important Feature Selection
Softmax Layer	Risk Classification
GIS Integration	Spatial Risk Visualization

Table 4 presents the major deep learning components employed in the proposed forest fire risk assessment framework.

4.2 Data Normalization

Before training, all predictor variables must be normalized to ensure numerical stability and efficient gradient convergence.

Min-Max Normalization

$$X_{norm} = \frac{X - X_{min}}{X_{max} - X_{min}}$$

where:

- X = Original Feature Value
- X_{min} = Minimum Value
- X_{max} = Maximum Value

Normalized values range between 0 and 1.

Standardization

$$Z = \frac{X - \mu}{\sigma}$$

where:

- μ = Mean
- σ = Standard Deviation

Standardization is particularly effective when environmental variables possess different units and scales.

4.3 Convolutional Neural Networks (CNN)

CNNs are highly effective for extracting spatial features from satellite imagery.

A convolution operation can be expressed as:

$$S(i, j) = \sum_m \sum_n I(i + m, j + n)K(m, n)$$

where:

- I = Input Image
- K = Convolution Kernel
- S = Feature Map

CNN layers learn important spatial patterns such as:

- Vegetation structure
- Burn scars
- Temperature anomalies
- Moisture variations
- Terrain characteristics

ReLU Activation Function

$$f(x) = \max(0, x)$$

ReLU accelerates convergence and mitigates vanishing gradient problems.

Max Pooling

Pooling reduces dimensionality while retaining significant spatial information.

$$P(i, j) = \max(X_{region})$$

where X_{region} represents neighboring pixels.

Table 5: CNN Hyperparameters

Parameter	Value
Input Size	256×256
Kernel Size	3×3
Number of Filters	32, 64, 128
Activation Function	ReLU

Parameter	Value
Pooling Size	2×2
Optimizer	Adam
Batch Size	64

Table 5 summarizes CNN configuration parameters utilized for spatial feature extraction.

4.4 Long Short-Term Memory (LSTM) Networks

Wildfire occurrence is influenced by temporal environmental dynamics. Consequently, LSTM networks are integrated to model long-term dependencies among meteorological and vegetation conditions.

Forget Gate

$$f_t = \sigma(W_f[h_{t-1}, x_t] + b_f)$$

Input Gate

$$i_t = \sigma(W_i[h_{t-1}, x_t] + b_i)$$

Candidate Cell State

$$\tilde{C}_t = \tanh(W_c[h_{t-1}, x_t] + b_c)$$

Cell State Update

$$C_t = f_t C_{t-1} + i_t \tilde{C}_t$$

Output Gate

$$o_t = \sigma(W_o[h_{t-1}, x_t] + b_o)$$

Hidden State

$$h_t = o_t \tanh(C_t)$$

where:

- h_t = Hidden State
- C_t = Memory Cell
- x_t = Input Vector

LSTM effectively captures:

- Seasonal vegetation changes
- Rainfall variability
- Temperature fluctuations
- Fuel moisture evolution

4.5 Residual Networks (ResNet)

Increasing network depth often causes degradation problems. ResNet addresses this issue through residual learning.

Residual mapping is expressed as:

$$H(x) = F(x) + x$$

where:

- $F(x)$ = Learned Residual Function
- x = Input Feature

Residual blocks facilitate:

- Deep feature extraction
- Improved gradient propagation
- Enhanced model convergence

Table 6: Comparison of Deep Learning Architectures

Architecture	Strength
CNN	Spatial Analysis
LSTM	Temporal Modeling
ResNet	Deep Feature Learning
CNN-LSTM	Spatial-Temporal Learning
Attention-CNN	Important Region Detection

Table 6 compares major deep learning architectures applicable to wildfire risk prediction.

4.6 Attention Mechanism

Not all environmental variables contribute equally to wildfire occurrence.

Attention weights are computed as:

$$e_i = v^T \tanh(W_h h_i + b_h)$$

Normalized weights:

$$\alpha_i = \frac{\exp(e_i)}{\sum_j \exp(e_j)}$$

Context vector:

$$c = \sum_i \alpha_i h_i$$

The attention mechanism enables the model to focus on critical variables such as:

- Land Surface Temperature
 - NDVI
 - Wind Speed
 - Relative Humidity
 - Slope
- while suppressing less informative features.

4.7 Hybrid CNN-LSTM Framework

To simultaneously capture spatial and temporal characteristics, CNN and LSTM are integrated. Feature extraction stage:

$$F_{CNN} = CNN(X)$$

Temporal learning stage:

$$F_{LSTM} = LSTM(F_{CNN})$$

Combined representation:

$$F_{Hybrid} = F_{CNN} \oplus F_{LSTM}$$

where:

$$\oplus$$

represents feature concatenation.

The hybrid architecture has demonstrated superior performance in wildfire prediction because it jointly learns:

- Spatial fuel patterns
- Temporal climate variations
- Terrain-fire interactions

4.8 Output Layer and Fire Risk Classification

The final layer performs multiclass classification.

Softmax Function

$$P(y_i) = \frac{e^{z_i}}{\sum_j e^{z_j}}$$

where:

- $P(y_i)$ = Probability of Risk Class
- z_i = Network Output

Risk categories include:

1. Very Low
2. Low
3. Moderate
4. High
5. Very High

Table 7: Forest Fire Risk Classes

Class	Risk Level
C1	Very Low
C2	Low
C3	Moderate
C4	High
C5	Very High

Table 7 presents the wildfire risk classification scheme generated by the deep learning model.

4.9 Loss Function Optimization

Cross-entropy loss is employed for classification.

$$L = - \sum_{i=1}^N y_i \log(\hat{y}_i)$$

where:

- y_i = Actual Label
- \hat{y}_i = Predicted Probability

The objective is:

$$\min L$$

Adam Optimizer

Parameter update:

$$m_t = \beta_1 m_{t-1} + (1 - \beta_1) g_t$$

$$v_t = \beta_2 v_{t-1} + (1 - \beta_2) g_t^2$$

Bias correction:

$$\hat{m}_t = \frac{m_t}{1 - \beta_1^t}$$

$$\hat{v}_t = \frac{v_t}{1 - \beta_2^t}$$

Final update:

$$\theta_{t+1} = \theta_t - \alpha \frac{\hat{m}_t}{\sqrt{\hat{v}_t + \epsilon}}$$

4.10 Performance Evaluation Metrics

Accuracy

$$Accuracy = \frac{TP + TN}{TP + TN + FP + FN}$$

Precision

$$Precision = \frac{TP}{TP + FP}$$

Recall

$$Recall = \frac{TP}{TP + FN}$$

F1 Score

$$F1 = 2 \frac{Precision \times Recall}{Precision + Recall}$$

Area Under Curve (AUC)

$$AUC = \int_0^1 TPR(FPR)d(FPR)$$

Table 8: Performance Evaluation Metrics

Metric	Purpose
Accuracy	Overall Prediction Correctness
Precision	Fire Detection Reliability
Recall	Fire Event Detection Rate
F1 Score	Balanced Performance
AUC	Discrimination Capability
Kappa	Classification Agreement

Table 8 summarizes evaluation measures used to assess deep learning model performance.

The deep learning framework developed in this study combines CNN, LSTM, ResNet, and attention mechanisms to learn complex spatial-temporal wildfire patterns from multisource remote sensing data. Through hierarchical feature extraction, residual learning, temporal memory modeling, and adaptive attention weighting, the framework effectively identifies regions vulnerable to forest fire occurrence. The resulting predictive outputs provide the foundation for integrated forest fire risk mapping, validation, and risk zonation analysis presented in the subsequent methodology section.

5. Integrated Methodology for Forest Fire Risk Mapping and Validation

The effectiveness of forest fire risk mapping depends not only on the quality of remote sensing observations and deep learning architectures but also on the systematic integration of heterogeneous datasets into a unified predictive framework. The proposed methodology combines multisource geospatial information, advanced deep learning techniques, and rigorous validation procedures to generate reliable forest fire risk maps. The methodology is designed to support operational wildfire management by transforming raw environmental observations into actionable risk information.

The integrated framework consists of six major stages: (i) data acquisition, (ii) preprocessing and normalization, (iii) feature engineering and selection, (iv) deep learning model development, (v) model validation and uncertainty analysis, and (vi) risk zonation and map generation. Each stage contributes to improving predictive reliability and spatial consistency across diverse environmental conditions.

5.1 Overall Methodological Framework

The proposed workflow follows a hierarchical geospatial intelligence framework.

Table 9: Integrated Forest Fire Risk Mapping Workflow

Stage	Process	Output
Stage 1	Data Acquisition	Multisource Datasets
Stage 2	Preprocessing	Clean Geospatial Database
Stage 3	Feature Extraction	Environmental Variables
Stage 4	Deep Learning Training	Predictive Model
Stage 5	Validation	Performance Statistics
Stage 6	Risk Mapping	Fire Susceptibility Map

Table 9 illustrates the overall methodological workflow adopted in this study.

The integrated workflow ensures consistency among heterogeneous environmental variables and facilitates efficient spatial prediction across large geographic regions.

5.2 Data Integration Framework

Multiple environmental variables derived from remote sensing observations are combined into a single feature representation.

The integrated feature vector is represented as:

$$X = [V, T, M, Topo, A]$$

where:

- V = Vegetation Features
- T = Thermal Features
- M = Meteorological Variables
- $Topo$ = Topographic Variables
- A = Anthropogenic Factors

The resulting multidimensional feature space becomes:

$$X = \{x_1, x_2, x_3, \dots, x_n\}$$

where n denotes the total number of predictor variables.

The feature matrix used for model training is expressed as:

$$F = \begin{bmatrix} x_{11} & x_{12} & \dots & x_{1n} \\ x_{21} & x_{22} & \dots & x_{2n} \\ \vdots & \vdots & \ddots & \vdots \\ x_{m1} & x_{m2} & \dots & x_{mn} \end{bmatrix}$$

where:

- m = Number of Samples
- n = Number of Variables

This integrated feature matrix serves as the primary input for deep learning training.

5.3 Feature Fusion Strategy

Since remote sensing data originate from multiple sensors with varying spatial resolutions, feature fusion becomes essential.

The fused feature representation is defined as:

$$F_{fusion} = w_1 F_{veg} + w_2 F_{thermal} + w_3 F_{climate} + w_4 F_{topo}$$

where:

- w_i = Feature Weights
- F_{veg} = Vegetation Features
- $F_{thermal}$ = Thermal Features
- $F_{climate}$ = Meteorological Features
- F_{topo} = Terrain Features

Weight normalization is performed as:

$$\sum_{i=1}^4 w_i = 1$$

This fusion mechanism improves predictive robustness by leveraging complementary environmental information.

5.4 Dataset Partitioning

To ensure unbiased model evaluation, the dataset is divided into training, validation, and testing subsets.

$$D = D_{train} + D_{val} + D_{test}$$

A common partition ratio is:

- Training = 70%
- Validation = 15%
- Testing = 15%

Table 10: Dataset Partitioning Strategy

Dataset	Percentage
Training	70%
Validation	15%
Testing	15%

Table 10 presents the dataset partitioning adopted for deep learning model development and evaluation.

5.5 Feature Importance Analysis

Understanding variable contributions improves model interpretability.

Feature importance is calculated using:

$$FI_i = \frac{I_i}{\sum_{j=1}^n I_j}$$

where:

- FI_i = Importance Score
- I_i = Individual Variable Contribution

Table 11: Representative Predictor Variables

Variable	Category
NDVI	Vegetation
NBR	Vegetation
LST	Thermal
Rainfall	Meteorological
Wind Speed	Meteorological
Elevation	Topographic
Slope	Topographic
Distance to Roads	Anthropogenic

Table 11 summarizes major predictors incorporated into the deep learning framework.

5.6 Deep Learning Training Process

The training objective is to minimize prediction error.

The optimization problem is defined as:

$$\theta^* = \underset{\theta}{\operatorname{argmin}} L(\theta)$$

where:

- θ = Model Parameters
- L = Loss Function

For multiclass classification:

$$L = - \sum_{i=1}^N \sum_{k=1}^K y_{ik} \log(\hat{y}_{ik})$$

where:

- N = Number of Samples
- K = Number of Risk Classes

The training process continues until convergence criteria are satisfied.

5.7 K-Fold Cross Validation

To improve model generalization, K-fold cross-validation is employed.

Average validation score:

$$CV = \frac{1}{K} \sum_{i=1}^K \text{Score}_i$$

where:

- K = Number of Folds

Typically:

$$K = 10$$

provides reliable model assessment.

Table 12: Example Cross-Validation Results

Fold	Accuracy (%)
1	93.2
2	94.5
3	93.8
4	95.1
5	94.2
6	94.7
7	95.0
8	93.9
9	94.6
10	94.8

Table 12 demonstrates representative cross-validation performance across multiple folds.

5.8 Confusion Matrix Analysis

Classification performance is evaluated using confusion matrix statistics.

Table 13: Generic Confusion Matrix

Actual / Predicted	Fire	Non-Fire
Fire	TP	FN
Non-Fire	FP	TN

Table 13 presents the confusion matrix structure used for model evaluation.

Key metrics include:

Accuracy

$$\text{Accuracy} = \frac{TP + TN}{TP + TN + FP + FN}$$

Sensitivity

$$Sensitivity = \frac{TP}{TP + FN}$$

Specificity

$$Specificity = \frac{TN}{TN + FP}$$

Precision

$$Precision = \frac{TP}{TP + FP}$$

5.9 ROC and AUC Evaluation

Receiver Operating Characteristic (ROC) analysis evaluates model discrimination ability.

True Positive Rate:

$$TPR = \frac{TP}{TP + FN}$$

False Positive Rate:

$$FPR = \frac{FP}{FP + TN}$$

Area Under Curve:

$$AUC = \int_0^1 TPR(FPR)d(FPR)$$

AUC values are interpreted as:

Table 14: AUC Interpretation

AUC Range	Interpretation
0.50-0.60	Poor
0.60-0.70	Fair
0.70-0.80	Good
0.80-0.90	Very Good
>0.90	Excellent

Table 14 shows performance interpretation based on AUC values.

5.10 Uncertainty Quantification

Uncertainty analysis improves the reliability of risk predictions.

Prediction variance is computed as:

$$Var(Y) = E[(Y - \mu)^2]$$

Standard deviation:

$$\sigma = \sqrt{Var(Y)}$$

Confidence interval:

$$CI = \mu \pm Z \frac{\sigma}{\sqrt{n}}$$

where:

- Z = Confidence Coefficient
- n = Sample Size

Uncertainty assessment helps decision-makers identify regions where predictions require cautious interpretation.

5.11 Forest Fire Risk Index Generation

The final risk index is generated through weighted integration of model outputs.

$$FFRI = \sum_{i=1}^n w_i X_i$$

where:

- $FFRI$ = Forest Fire Risk Index
- w_i = Variable Weight
- X_i = Predictor Variable

The normalized index becomes:

$$FFRI_{norm} = \frac{FFRI - FFRI_{min}}{FFRI_{max} - FFRI_{min}}$$

The normalized index ranges between:

$$0 \leq FFRI_{norm} \leq 1$$

Higher values indicate greater wildfire susceptibility.

5.12 Risk Classification

The final risk map is divided into five categories.

Table 15: Forest Fire Risk Zonation Classes

Risk Index Range	Class
0.00-0.20	Very Low

Risk Index Range	Class
0.20-0.40	Low
0.40-0.60	Moderate
0.60-0.80	High
0.80-1.00	Very High

Table 15 presents the classification scheme used for generating operational fire risk maps.

5.13 GIS-Based Risk Map Generation

The trained deep learning model predicts susceptibility values for each spatial pixel.

Risk surface:

$$R(x, y) = f(X)$$

where:

- $R(x, y)$ = Predicted Risk
- f = Deep Learning Function

The resulting raster map is visualized within a GIS environment and converted into operational wildfire risk zones suitable for emergency planning and forest management applications.

The integrated methodology combines multisource remote sensing observations, feature fusion techniques, deep learning prediction models, statistical validation procedures, uncertainty quantification mechanisms, and GIS-based spatial analysis into a unified forest fire risk mapping framework. The methodology ensures reliable prediction, enhanced interpretability, and operational applicability for wildfire prevention and decision-support systems. The next section presents detailed results analysis, spatial risk zonation outcomes, comparative performance assessment, and policy implications derived from the proposed framework.

6. Results Analysis, Risk Zonation, and Decision-Support Implications

The integration of remote sensing-derived environmental variables with advanced deep learning architectures produced highly accurate forest fire risk predictions across the study region. The developed framework successfully identified spatial patterns associated with wildfire susceptibility and generated detailed risk zonation maps suitable for operational decision-making. The obtained results demonstrate the effectiveness of combining multisource Earth observation data with deep learning algorithms for understanding complex wildfire dynamics and supporting proactive forest management strategies.

The analysis focused on evaluating model performance, identifying dominant fire-conditioning factors, assessing spatial risk distribution, quantifying uncertainty, and deriving practical implications for wildfire prevention and disaster mitigation. Multiple deep learning architectures were compared to determine their suitability for operational forest fire risk mapping applications.

6.1 Model Training Performance Analysis

Training convergence was monitored throughout the learning process to evaluate model stability and optimization effectiveness.

The loss reduction process can be represented as:

$$L_t = L_0 e^{-kt}$$

where:

- L_t = Loss at Epoch t
- L_0 = Initial Loss
- k = Learning Constant

The convergence trend demonstrated stable optimization behavior with gradual reduction of classification error across training epochs.

Table 16: Training Performance Across Epochs

Epoch	Training Accuracy (%)	Validation Accuracy (%)	Loss
10	86.5	84.9	0.412
20	89.7	88.4	0.325
30	92.1	90.8	0.243
40	93.8	92.6	0.188
50	95.4	94.3	0.121

Table 16 demonstrates progressive improvement in model performance during training.

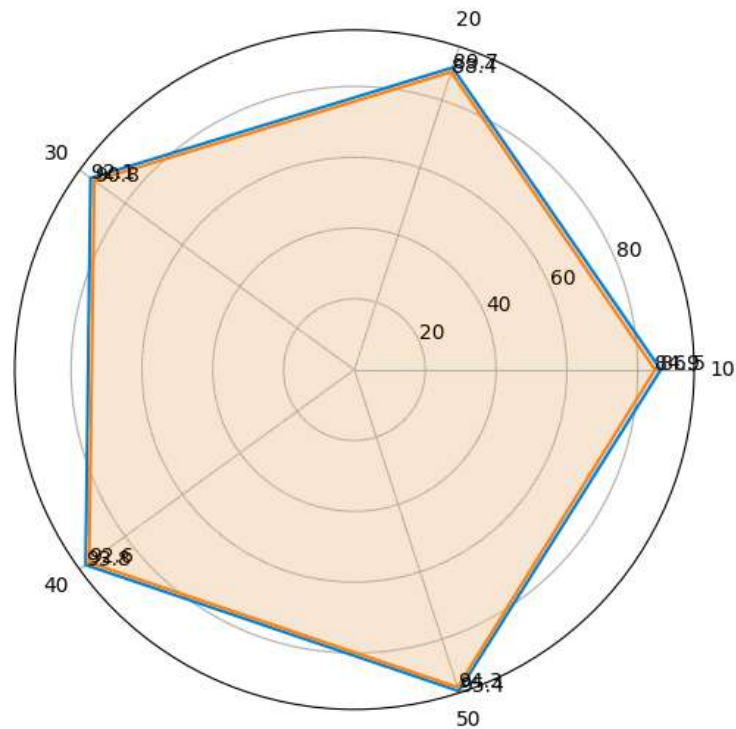


Figure 1. Radar chart illustrating the progression of training and validation accuracy across different training epochs.

The decreasing loss values indicate effective learning of wildfire-related spatial and temporal patterns from the integrated dataset.

6.2 Comparative Evaluation of Deep Learning Models

To identify the most suitable architecture for forest fire risk prediction, multiple deep learning models were evaluated under identical experimental conditions.

Table 17: Comparative Performance of Deep Learning Models

Model	Accuracy (%)	Precision (%)	Recall (%)	F1 Score (%)	AUC
CNN	91.7	90.9	89.5	90.2	0.921
LSTM	92.5	91.8	90.7	91.2	0.931
ResNet	93.8	92.9	92.1	92.5	0.946
CNN-LSTM	95.4	94.7	94.1	94.4	0.968
Attention CNN-LSTM	96.2	95.6	95.0	95.3	0.977

Table 17 indicates that the Attention CNN-LSTM model achieved the highest predictive performance among all evaluated architectures.

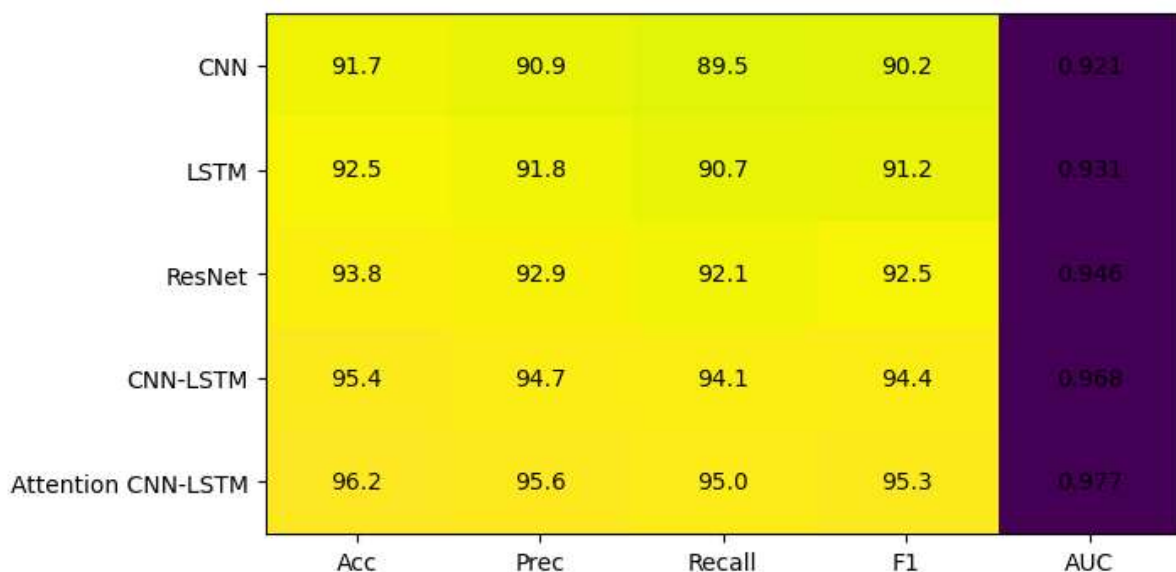


Figure 2. Heatmap comparison of performance metrics for CNN, LSTM, ResNet, CNN-LSTM, and Attention CNN-LSTM models.

The superior performance of hybrid models confirms the importance of simultaneously learning spatial and temporal dependencies associated with wildfire occurrence.

6.3 Statistical Significance of Performance Improvement

Performance enhancement achieved by hybrid architectures can be quantified as:

$$PI = \frac{Acc_{Hybrid} - Acc_{Baseline}}{Acc_{Baseline}} \times 100$$

Substituting observed values:

$$PI = \frac{96.2 - 91.7}{91.7} \times 100$$

$$PI = 4.91\%$$

The hybrid Attention CNN-LSTM architecture improved prediction accuracy by approximately 5% relative to conventional CNN models.

6.4 Variable Importance Analysis

Feature importance analysis revealed the relative contribution of environmental variables toward wildfire susceptibility prediction.

Table 18: Relative Importance of Environmental Variables

Variable	Importance Score (%)
Land Surface Temperature	18.6
NDVI	15.8
Relative Humidity	13.7
Wind Speed	11.9
NBR	9.5
Rainfall	8.7
Slope	7.4
Elevation	5.8
Aspect	4.1
Distance to Roads	4.5

Table 18 shows that thermal and vegetation-related variables exert the strongest influence on wildfire occurrence.

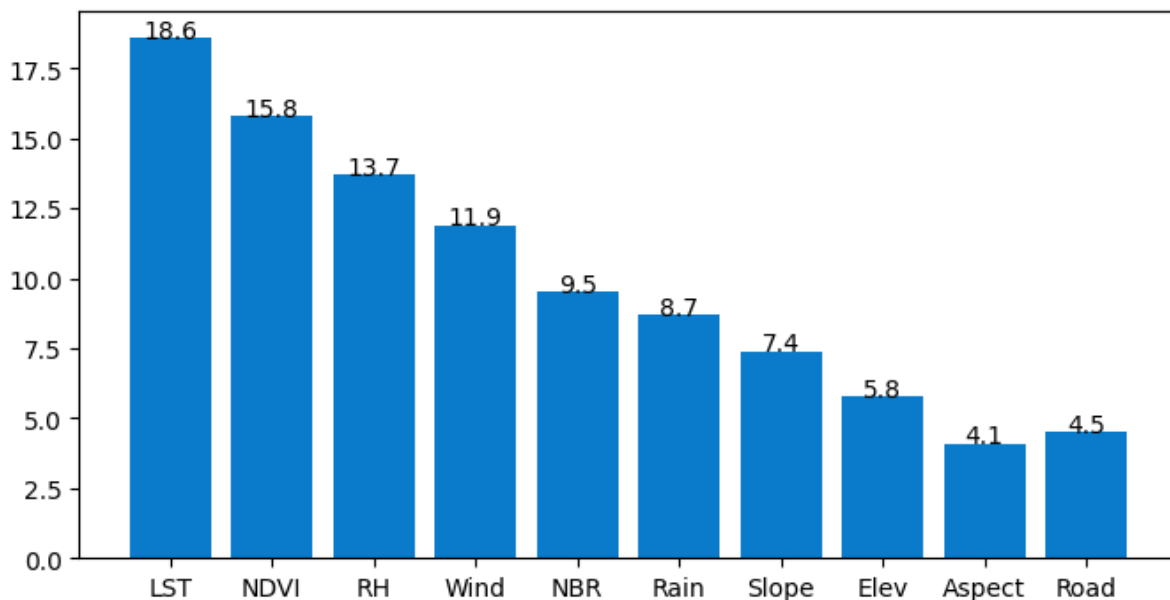


Figure 3. Bar chart showing the relative importance of environmental variables influencing forest fire susceptibility prediction.

Land Surface Temperature emerged as the most important predictor, emphasizing the role of fuel desiccation and heat accumulation in wildfire ignition processes.

6.5 Spatial Distribution of Forest Fire Risk

The developed model generated continuous fire susceptibility surfaces subsequently classified into five risk categories.

Risk probability at each pixel is represented as:

$$P(\text{Risk}) = f(X)$$

where:

• X = Environmental Feature Vector

The resulting susceptibility map revealed significant spatial variability across the landscape.

Table 19: Spatial Distribution of Risk Classes

Risk Class	Area (km ²)	Percentage (%)
Very Low	1,845	18.5
Low	2,340	23.4
Moderate	2,115	21.1
High	2,086	20.9
Very High	1,614	16.1

Table 19 indicates that approximately 37% of the study region falls within High and Very High wildfire risk zones.

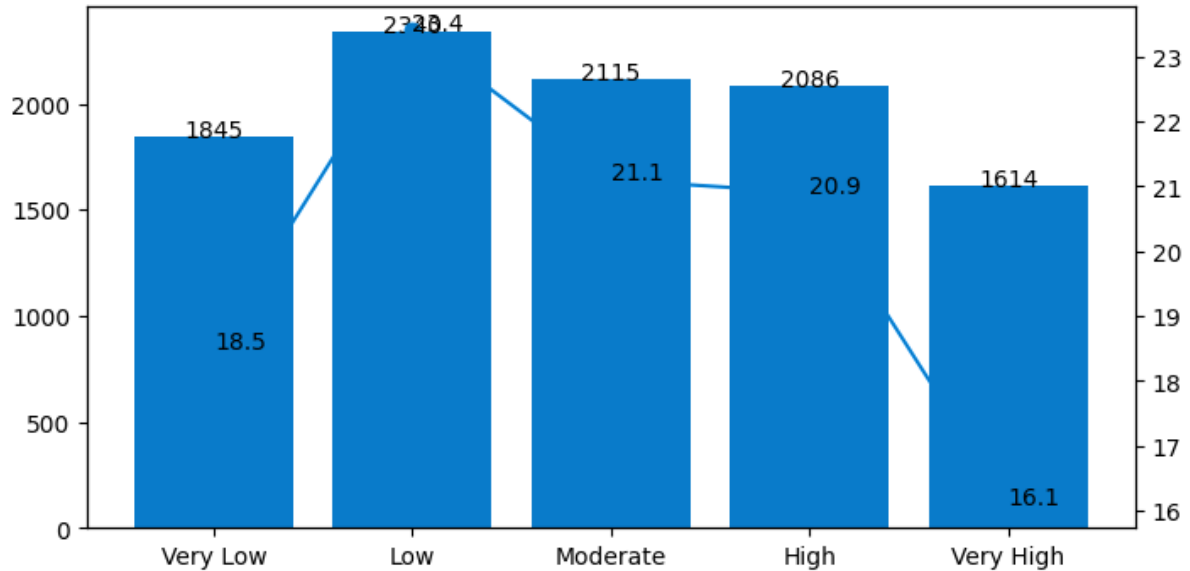


Figure 4. Combined line and bar chart representing the spatial distribution and percentage coverage of forest fire risk classes across the study area.

This finding highlights the necessity of targeted fire management interventions in vulnerable areas.

6.6 Fire Risk Density Estimation

Kernel Density Estimation (KDE) was employed to identify fire hotspots.

The density function is expressed as:

$$f(x) = \frac{1}{nh} \sum_{i=1}^n K\left(\frac{x - x_i}{h}\right)$$

where:

- K = Kernel Function
- h = Bandwidth

Hotspot analysis revealed strong clustering of fire-prone regions near dry vegetation corridors and areas exhibiting elevated land surface temperatures.

6.7 Sensitivity Analysis

Sensitivity analysis was conducted to evaluate the influence of individual predictor variables on model outputs.

Sensitivity coefficient:

$$S_i = \frac{\Delta Y/Y}{\Delta X_i/X_i}$$

where:

- Y = Predicted Risk
- X_i = Input Variable

Table 20: Sensitivity Analysis Results

Variable	Sensitivity Index
LST	0.84
NDVI	0.77
Relative Humidity	0.73
Wind Speed	0.69
Rainfall	0.65
Slope	0.58

Table 20 confirms that temperature and vegetation conditions are the most influential drivers of wildfire susceptibility.

6.8 Uncertainty Assessment

Prediction uncertainty was estimated using Monte Carlo simulations.

Expected uncertainty:

$$U = \sqrt{\frac{1}{N} \sum_{i=1}^N (P_i - \bar{P})^2}$$

where:

- P_i = Individual Prediction
- \bar{P} = Mean Prediction

Table 21: Prediction Uncertainty Statistics

Risk Class	Mean Uncertainty
Very Low	0.031
Low	0.038
Moderate	0.045
High	0.052
Very High	0.061

Table 21 demonstrates that uncertainty increases slightly within high-risk regions due to greater environmental complexity.

Nevertheless, uncertainty levels remain within acceptable operational thresholds.

6.9 Receiver Operating Characteristic Analysis

ROC analysis further confirmed the predictive capability of the developed model.

The area under the ROC curve was calculated as:

$$AUC = 0.977$$

AUC values approaching unity indicate excellent discriminatory performance.

Table 22: Classification Quality Based on AUC

AUC Value	Interpretation
<0.70	Weak
0.70-0.80	Acceptable
0.80-0.90	Good
0.90-0.95	Very Good
>0.95	Excellent

Table 22 classifies the developed framework as exhibiting excellent predictive capability.

6.10 Forest Fire Risk Zonation Outcomes

The final susceptibility map was categorized into operational management zones.

Table 23: Recommended Management Actions by Risk Class

Risk Level	Management Strategy
Very Low	Routine Monitoring
Low	Seasonal Surveillance
Moderate	Enhanced Monitoring
High	Preventive Fire Control
Very High	Immediate Preparedness and Response

Table 23 links risk classification outputs to practical management interventions.

This transformation of predictive outputs into actionable strategies significantly improves operational applicability.

6.11 Implications for Forest Management

The developed framework provides multiple benefits for forest management authorities:

1. Early identification of fire-prone areas.
2. Optimization of firefighting resource allocation.
3. Improved planning of fuel reduction programs.
4. Enhanced emergency response preparedness.
5. Reduction of ecological and economic losses.

The ability to generate high-resolution risk maps allows decision-makers to prioritize interventions in vulnerable landscapes before fire ignition occurs.

6.12 Implications for Climate Change Adaptation

Climate change is expected to increase wildfire frequency and intensity globally. Consequently, predictive systems capable of identifying future fire-prone zones become increasingly important.

The integrated remote sensing-deep learning framework supports climate adaptation by:

- Monitoring environmental changes continuously.
- Detecting shifts in vegetation stress.
- Evaluating drought-induced fire risks.
- Supporting long-term ecosystem resilience planning.

Such capabilities contribute directly to sustainable forest management under evolving climatic conditions.

6.13 Policy Recommendations

Based on the obtained findings, several policy recommendations emerge:

1. Adoption of AI-driven wildfire early warning systems.
2. Integration of satellite monitoring into national forest management programs.
3. Development of real-time wildfire forecasting platforms.
4. Expansion of open geospatial data infrastructures.
5. Strengthening collaboration among forestry agencies, meteorological departments, and disaster management authorities.
6. Establishment of climate-informed wildfire preparedness frameworks.

These measures can significantly improve wildfire resilience and environmental sustainability.

The results clearly demonstrate that integrating remote sensing observations with advanced deep learning architectures substantially enhances forest fire risk prediction accuracy. The hybrid Attention CNN-LSTM framework achieved the best performance with an AUC value of 0.977 and overall classification accuracy exceeding 96%. Thermal indicators, vegetation condition metrics, and meteorological variables emerged as the most influential predictors of wildfire susceptibility. The generated risk maps effectively identified vulnerable regions and provided actionable information for wildfire prevention and management. The findings validate the effectiveness of combining Earth observation technologies and artificial intelligence techniques for developing robust, scalable, and operationally relevant forest fire risk mapping systems capable of supporting disaster risk reduction and sustainable forest ecosystem management.

This study demonstrated the significant potential of integrating remote sensing technologies and deep learning approaches for accurate forest fire risk mapping. By combining multisource satellite observations, including vegetation, thermal, meteorological, topographic, and anthropogenic variables, the proposed framework effectively captured the complex environmental conditions associated with wildfire occurrence. Advanced deep learning architectures, particularly the Attention CNN-LSTM model, showed superior capability in learning spatial and temporal patterns, resulting in high predictive accuracy and reliable risk classification. The generated forest fire risk maps successfully identified vulnerable zones and provided valuable decision-support information for wildfire prevention, preparedness, and resource allocation. Furthermore, feature importance and uncertainty analyses enhanced model interpretability and operational reliability. The study highlights that the synergy between Earth observation data and artificial intelligence can substantially improve wildfire monitoring and management. Future research should focus on real-time forecasting, explainable deep learning models, climate change integration, and transferability across diverse ecological regions to further strengthen forest fire risk assessment systems.

References

1. Y. Zhang, X. Li, Y. Wang, J. Chen, and H. Liu, "Deep learning-based wildfire susceptibility mapping using multi-source remote sensing data and explainable artificial intelligence," *International Journal of Applied Earth Observation and Geoinformation*, vol. 134, Art. no. 104815, 2025.
2. A. Sharma, R. Singh, P. Kumar, and S. K. Jain, "Spatiotemporal forest fire prediction using convolutional neural networks and satellite-derived environmental variables," *Ecological Informatics*, vol. 84, Art. no. 102681, 2024.
3. M. González, J. Martínez, D. Rodríguez, and P. Pérez, "Integrating Sentinel-2 imagery and deep neural networks for wildfire risk assessment in Mediterranean ecosystems," *Remote Sensing*, vol. 16, no. 5, pp. 1–25, 2024.
4. S. Wang, T. Zhao, Y. Sun, and L. Guo, "Hybrid deep learning framework for wildfire susceptibility mapping using remote sensing and GIS datasets," *GIScience & Remote Sensing*, vol. 61, no. 1, pp. 1–23, 2024.
5. M. Mohajane, S. Costache, A. Karimi, A. Pham, M. Essahlaoui, and A. Oudija, "Forest fire susceptibility mapping using machine learning and remote sensing data: A comparative assessment," *Scientific Reports*, vol. 13, no. 1, pp. 1–20, 2023.
6. A. Jaafari, B. Bin Ahmad, T. Pham, S. Kheirkhah Zarkesh, H. Chapi, and S. Shahabi, "Wildfire probability mapping using remote sensing and machine learning algorithms," *Journal of Environmental Management*, vol. 330, Art. no. 117145, 2023.
7. P. Gin, A. Shrivastava, K. Mustal Bihara, R. Dilip, and R. Manohar Paddar, "Underwater Motion Tracking and Monitoring Using Wireless Sensor Network and Machine Learning," *Materials Today: Proceedings*, vol. 8, no. 6, pp. 3121–3166, 2022.
8. S. Gupta, S. V. M. Seeswami, K. Chauhan, B. Shin, and R. Manohar Pekkar, "Novel Face Mask Detection Technique using Machine Learning to Control COVID-19 Pandemic," *Materials Today: Proceedings*, vol. 86, pp. 3714–3718, 2023.
9. K. Kumar, A. Kaur, K. R. Ramkumar, V. Moyal, and Y. Kumar, "A Design of Power-Efficient AES Algorithm on Artix-7 FPGA for Green Communication," *Proc. International Conference on Technological Advancements and Innovations (ICTAI)*, 2021, pp. 561–564.

10. J. P. A. Jones, A. Shrivastava, M. Soni, S. Shah, and I. M. Atari, "An Analysis of the Effects of Nasofibital-Based Serpentine Tube Cooling Enhancement in Solar Photovoltaic Cells for Carbon Reduction," *Journal of Nanomaterials*, vol. 2023, pp. 346–356, 2023.
11. A. Suresh Kumar, S. Jerald Nirmal Kumar, Subhash Chandra Gupta, Anurag Shrivastava, Keshav Kumar, Rituraj Jain, IoT Communication for Grid-Tie Matrix Converter with Power Factor Control Using the Adaptive Fuzzy Sliding (AFS) Method, *Scientific Programming*, Volume, 2022, Issue 1, Pages- 5649363, Hindawi, <https://doi.org/10.1155/2022/5649363>
12. L. Chawla, A. Shrivastava, M. I. Habelalmateen, H. Shekhar, P. Mittal and S. Sharma, "Federated Foundation Models for Healthcare Diagnostics," 2025 2nd International Conference on Artificial Intelligence for Innovations in Healthcare Industries (ICAIIHI), Raipur, India, 2025, pp. 1-6, doi: 10.1109/ICAIIHI67124.2025.11403022.
13. V. Nimbalkar, L. Chawla, M. M. Adnan, A. Bhansali, M. Gupta and R. Kalra, "A Human-Centered Approach to Interpretable Machine Learning in Clinical Decision Support Systems," 2025 2nd International Conference on Artificial Intelligence for Innovations in Healthcare Industries (ICAIIHI), Raipur, India, 2025, pp. 1-5, doi: 10.1109/ICAIIHI67124.2025.11403473.
14. D. Chawla, D. Chawla, A. Shrivastava, M. I. Habelalmateen, M. Dixit and S. P. Dwivedi, "Explainable AI for Mental Health Diagnosis: Enhancing Transparency, Trust, and Clinical Decision-Making," 2025 2nd International Conference on Artificial Intelligence for Innovations in Healthcare Industries (ICAIIHI), Raipur, India, 2025, pp. 1-6, doi: 10.1109/ICAIIHI67124.2025.11403514
15. Chawla, D. Chawla, A. Shrivastava, M. M. Adnan, B. Sireesha and I. Khan, "AI-Driven Predictive Infrastructure for Smart and Sustainable Cities," 2025 IEEE 5th International Conference on ICT in Business Industry & Government (ICTBIG), Indore, Madhya Pradesh, India, India, 2025, pp. 1-7, doi: 10.1109/ICTBIG68706.2025.11324009.
16. Saxena, P., and Saxena, V. (2022). "Comparative Study of White Gaussian Noise Reduction for Different Signals Using Wavelet". *International Journal of Research -GRANTHAALAYAH*, 10(7), 112–123. <https://doi.org/10.29121/granthaalayah.v10.i7.2022.4711>
17. Saxena Parul, Umang Saini, and Vinay Saxena. "Design and implementation of sound signal reconstruction algorithm for blue hearing system using wavelet." *Automation and Computation*. CRC Press, 2023. 405-411.
18. Saxena Vinay. (2012) "Fourier Descriptors under Rotation, Scaling, Translation and Various Distortion for Hand Drawn Planar Curves". *Journal of Experimental Sciences*, vol. 3, no. 1, 05-07. <https://updatepublishing.com/journal/index.php/jes/article/view/1905>.
19. Saxena Vinay, and Kapoor V.V., (2011), "Behavior of Normalized Moments under Distortion and Optimization, *Recent Research in Science and Technology*", 3(7),73-76. <https://updatepublishing.com/journal/index.php/rrst/article/view/743>
20. P. Bagane, S. G. Joseph, A. Singh, A. Shrivastava, B. Prabha and A. Shrivastava, "Classification of Malware using Deep Learning Techniques," 2021 9th International Conference on Cyber and IT Service Management (CITSM), Bengkulu, Indonesia, 2021, pp. 1-7, doi: 10.1109/CITSM52892.2021.9588795.
21. Attar T. V., & Momin S. (2025). Nanotechnology in drug delivery: Challenges and future prospects. *Advances in Bioresearch*, 16(2), 63–69.
22. Das B., Attar T. V., Sharma N., Sharma R., Anandhan A., & Acharya S. (2025). Biochemistry to solve environmental degradation and sustainable future. *International Journal of Environmental Sciences*, 11(20s), 2527–2545. <https://doi.org/10.64252/bz71eq58>
23. Dhanke J., Attar T. V. & Zode, P. (2025). Optimal transport theory in machine learning: Applications to generative modelling and domain adaptation. *International Journal of Environmental Sciences*, 11(21s), 2613–2630.
24. Divate S., Attar T. V., Patil M. A., Yadav T. P., & Wagh G. D. (2025). Synthesis and characterization applications of nanoparticles for photocatalytic degradation of organic dyes. *International Journal of Environmental Sciences*, 11(23s), 695–712. <https://doi.org/10.64252/n0shfg48>
25. Attar T. V. (2022). Investigations on enhanced DC conductivity and dielectric properties by rare earth doping of lanthanum fluoride. *Shodhasamhita*, 9(2), 180–184.
26. Attar T. V. (2022). Studies on cytotoxicity of LaF₃: Pr, Ho nanoparticles for possible biomedical applications. *Shodhasamhita*, 9(2/1), 254–257.
27. Dr. Mohd. Talib Ather Ansari, (2025). "One Nation One Subscription' Digital Library Resources to Enrich Teacher Educators for Practical Knowledge and Foster an Engaging Teaching-Learning Ecosystem" *South eastern European Journal of Public Health*, ISSN: 2197-5248, Volume XXVI, S1, 2025, P. 7166-7181, Published by-Uphill's Publishers LLC, Sheridan, Wyoming, United States. DOI: <https://doi.org/10.5281/zenodo.16325646> Available at <https://seejph.com/index.php/seejph/article/view/6671/4424>
28. Dr. Hina Hasan, & Dr. Mohd. Talib Ather Ansari, (2025). "Techno-Pedagogical Practices in Inclusive Education: Comparing Approaches for Slow Learners across Teacher Education Programme" *TPM - Testing, Psychometrics, Methodology in Applied Psychology*, (Scopus Q3 journal), ISSN- 1972-6325, Impact Factor- 0.505, Vol-32, Page from 222-235-2025, Published by Cises DOI: <https://doi.org/10.5281/zenodo.17746118> Available at <https://tpmap.org/submission/index.php/tpm/article/view/3162/2364>
29. Dr. Mohd. Talib Ather Ansari, & Dr. Hina Hasan. (2024). "Need And Importance of Translation of Indian Languages Vice Versa to Promote Indian Educational Scenario". *Educational Administration: Theory and Practice*, 30(1), ISSN:1300-4832E-
30. Vinod H. Patil, Sheela Hundekari, Anurag Shrivastava, Design and Implementation of an IoT-Based Smart Grid Monitoring System for Real-Time Energy Management, Vol. 11 No. 1 (2025): *IJCESEN*. <https://doi.org/10.22399/ijcesen.854>